Journal of Power Sources 196 (2011) 10222–10227

Contents lists available at SciVerse ScienceDirect

Journal of Power Sources

journal homepage: www.elsevier.com/locate/jpowsour

$LiCr_{0.2}Ni_{0.4}Mn_{1.4}O_4$ spinels exhibiting huge rate capability at 25 and 55 °C: Analysis of the effect of the particle size

Mohamed Aklalouch[a,b], José Manuel Amarilla[a,*], Ismael Saadoune[b], José María Rojo[a]

[a] Instituto de Ciencia de Materiales de Madrid, Consejo Superior de Investigaciones Científicas (CSIC), c/Sor Juana Inés de la Cruz, 3 28049 Madrid, Spain
[b] ECME, Faculté des Sciences et Techniques Marrakech, Université Cadi Ayyad, Av. A. ElKhattabi, B.P.549 Marrakech, Morocco

ARTICLE INFO

Article history:
Received 13 June 2011
Received in revised form 28 July 2011
Accepted 16 August 2011
Available online 22 August 2011

Keywords:
Lithium battery
5 V cathode material
Rate capability
Particle size
$LiMn_2O_4$-based cathodes
$LiNi_{0.5}Mn_{1.5}O_4$ spinel

ABSTRACT

The comparison of the rate capability of $LiCr_{0.2}Ni_{0.4}Mn_{1.4}O_4$ spinels synthesized by the sucrose aided combustion method at 900, 950 and 1000 °C is presented. XRD and TEM studies show that the spinel cubic structure remains unchanged on heating but the particle size is notably modified. Indeed, it increases from 695 nm at 900 °C to 1465 nm at 1000 °C. The electrochemical properties have been evaluated by galvanostatic cycling at 25 and 55 °C between 1 C and 60 C discharge rates. At both temperatures, all samples exhibit high working voltage (~4.7 V), elevated capacity (~140 mAh g^{-1}) and high cyclability (capacity retention ~99% after 50 cycles even at 55 °C). The samples also have huge rate capability. They retain more than 70% of their maximum capacity at the very fast rate of 60 C. The effect of the particle size on the rate capability at 25 and at 55 °C has been investigated. It was demonstrated that $LiCr_{0.2}Ni_{0.4}Mn_{1.4}O_4$ annealed at 900 °C, with the lowest particle size, has the best electrochemical performances. In fact, among the $LiNi_{0.5}Mn_{1.5}O_4$-based cathodes, SAC900 exhibits the highest rate capability ever published. This spinel, able to deliver 31,000 W kg^{-1} at 25 °C and 27,500 W kg^{-1} at 55 °C is a really promising cathode for high-power Li-ion battery.

1. Introduction

The electrification of the road transport, i.e. the wide use of electric vehicles (EVs), is one of the more straightforward ways to combat three of the most important challenges of the XXI century: (i) climatic change, (ii) increased pollution in large cities and (iii) strong dependence on fossil fuels. A key factor for EVs is the battery which must combine high energy and power with low pollution and cost [1]. Nowadays, lithium-ion batteries (LIBs) are the technology of choice to drive the EVs [1–3]. A major challenge in LIBs is to develop new electrode materials with power capabilities close to that of supercapacitors (~10 kW kg^{-1}) [4–6]. To reach this goal, several strategies are being developed. For instance (i) doping popular electrode materials such as $LiCoO_2$ [7,8] and $LiMn_2O_4$ [9,10], (ii) coating the active materials such as carbon coated $LiFePO_4$ [5,11] or ZnO coated $LiNi_{0.5}Mn_{1.5}O_4$ spinel [12] and (iii) tailoring the particle size of the electrode materials [2,3,13–15]. Probably, the latter strategy is the most followed because it has been widely demonstrated that the power output of LIBs can be notably increased by reducing the particle size, i.e. decreasing the Li^+-diffusion pathways.

Among the cathode materials under study, $LiMn_2O_4$ type spinels (LMS) are one of the most promising candidates for the large-size LIBs needed for electrical vehicles. The main advantages are their low cost and environment friendliness [1,9,16,17]. LMS-type oxydes have a cubic spinel structure, space group Fd-3 m [9,17,18]. It can be described as a close-cubic packed of O^{2-} anions in which the Li^+ cations are placed in the 8a tetrahedral positions and the manganese and dopant metal cations (M) are situated in the 16d octahedral sites. The $[Mn,M]_2O_4$ framework defines a three-dimensional network of channels through which the Li^+ cations can be reversibly de-/inserted. Among the LMS-types cathodes, those derived of the spinel $LiNi_{0.5}Mn_{1.5}O_4$ (LNMS) has been intensively studied since Zhong et al. [19] showed that LNMS was able to de-/inserted Li^+ ions at very high potential (~4.7 V vs. Li^+/Li) [20–23]. Moreover, LNMS-type cathodes show high reversible capacities (~135 mAh g^{-1}) at room temperature [21,24,25]. Unfortunately, the electrochemical performances of these cathodes notably worsen at elevated temperature (~55 °C) [12,22,26,27]. The development of new strategies to overcome this serious drawback is nowadays one of the most active research lines in the field of advanced cathodes for LIBs. We showed that it is possible to enhance the electrochemical performance of LNMS by doping with chromium. Among the $LiCr_{2y}Ni_{0.5-y}Mn_{1.5-y}O_4$ spinels synthesized, the sample with $y = 0.1$ ($LiCr_{0.2}Ni_{0.4}Mn_{1.4}O_4$) exhibited the best electrochemical performances [28]. Furthermore, we

* Corresponding author. Tel.: +34 91 334 90 74; fax: +34 91 372 06 23.
E-mail address: amarilla@icmm.csic.es (J.M. Amarilla).

0378-7753/$ – see front matter © 2011 Elsevier B.V. All rights reserved.
doi:10.1016/j.jpowsour.2011.08.069

demonstrated that cycleability at 25 and at 55 °C of the $LiCr_{0.2}Ni_{0.4}Mn_{1.4}O_4$ spinel strongly depended on the particle size [27]. The samples synthesized at $T \geq 900$ °C, with particle size >690 nm, shown a remarkable cycling performance even when cycling was performed at elevated temperature (55 °C). In this paper, we report the effect of particle size of the $LiCr_{0.2}Ni_{0.4}Mn_{1.4}O_4$ spinel annealed at $T \geq 900$ °C on its rate capability and its specific power at 25 and 55 °C.

2. Experimental/materials and methods

The "as-prepared" $LiCr_{0.2}Ni_{0.4}Mn_{1.4}O_4$ spinel was synthesized by the sucrose aided combustion method previously described [28]. Three $LiCr_{0.2}Ni_{0.4}Mn_{1.4}O_4$ samples have been prepared by annealing for 1 h the "as-prepared" spinel at 900, 950 and 1000 °C being the heating/cooling rate of 2 °C min^{-1}. The samples are labeled as "SACNumber" where SAC and Number stand for Sucrose Aided Combustion and for the annealing temperature, respectively.

The analysis of the phase purity and the structural characterization were made by X-ray powder diffraction (XRD) using a Bruker D8 diffractometer equipped with a Super Speed Vantec-1 detector, and Cu Kα radiation.

The morphological characterization of the SAC-samples was carried out by transmission electron microscopy (TEM) using a Jeol 2000 FX microscope operating at an acceleration voltage of 200 kV. The samples were dispersed in *n*-butyl alcohol by ultrasound and then, drops were transferred to a carbon-coated copper grid. To determine the particle size of the samples, more than 20 micrographs were taken for each sample in different regions of the holder grid. The TEM images were analyzed with the commercial software IMAGEJ [29].

The rate capability studies were performed at 25 and 55 °C with an Arbin-BT4 battery system. Positive electrode composites were prepared by dispersing into acetone the active material (72 wt.%) with MMM Super-P carbon black (20 wt.%) and poly(vinylidenefluorine-co-hexafluoropropylene) Kynar Flex® 2801 (8 wt.%). The slurry was pasted on an Al foil and dried at 80 °C overnight. Discs of 1.2 cm in diameter, containing 1.8 ± 0.4 mg of SAC-spinels (1.6 mg cm^{-2}) were cut. CR2032 coin cells were assembled using Li metal as negative electrode and 1 M $LiPF_6$ in EC:DMC (1:1 in volume) as electrolyte. Cycling galvanostatic measurements were conducted under thermostatic conditions at 25 ± 0.5 and at 55 ± 1 °C. The cells were cycled at discharge rates from 1 C to 60 C (1 C = 147.5 mA g^{-1} or 0.260 mA cm^{-2}) and 0.5 C charge current. After the rate capability study, the cells were subjected to cycle back at the lower rate (1 C) for two cycles to test if the reduction of capacity at the highest rates is reversible. The upper cut-off potential was 5.2 V and the lower one was gradually decreased from 3.4 V for 1 C to 2.5 V for 60 C to compensate from the ohmic voltage drop caused by the cell impedance. All over the manuscript, capacity, energy and power are refereed to mass of $LiCr_{0.2}Ni_{0.4}Mn_{1.4}O_4$ in the composite cathode.

3. Result and discussion

The structural characterization of the SAC-samples was carried out by X-ray diffraction. The corresponding patterns, given in Fig. 1, indicate that single phase spinels were obtained for the three annealing temperatures. The absence of the (2 2 0) diffraction peak around $2\theta = 30°$ indicates that there is no transition metal ions in the 8a tetrahedral positions. The cubic unit cell parameter (a_c) for the SAC-spinels is summarized in Table 1. The likeness of the a_c-values indicates that the cubic spinel structure is preserved on heating.

The morphology and the particle size of the SAC-spinels have been investigated by transmission electron microscopy. As an example, TEM micrographs of SAC950 and SAC1000 samples are shown in Fig. 2. It was observed that the particles are homogeneous in size and exhibit well defined faces. Furthermore, the sharp edges of the particles evidence the high crystallinity of the studied SAC-spinels which agree with the X-ray results. The analysis of the TEM pictures clearly shows that particle size notably increases on heating. Particle size was determined from many different TEM micrographs. As an example, Fig. 2c shows the histograms for SAC950. The particle size together with the standard deviation was calculated from the Gaussian fit. The best fitting is also drawn in the same figure. Values of the average particle size together with the corresponding standard deviation are summarized in Table 1. As shown, the particle size notably increases from 695 to 1465 nm when the annealing temperature was increased from 900 to 1000 °C. In summary, the main conclusions deduced from the characterization studies are: (i) the cubic spinel structure remains unchanged from 900 to 1000 °C, and (ii) the particle size notably increases on heating.

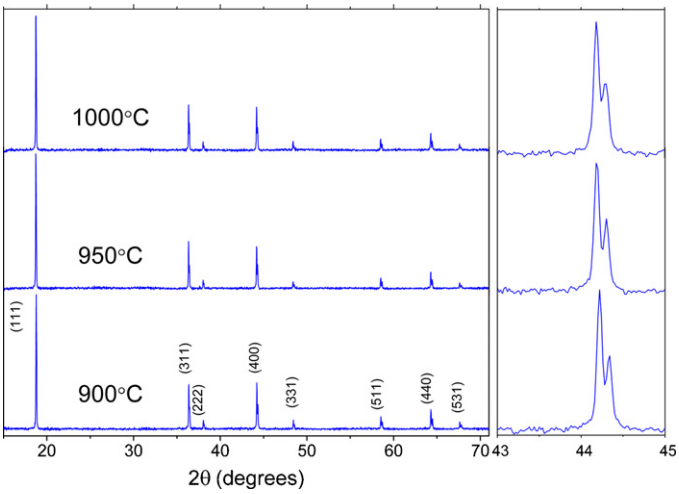

Fig. 1. X-ray diffraction patterns of $LiCr_{0.2}Ni_{0.4}Mn_{1.4}O_4$ spinels annealed at the indicated temperatures. The right part of the figure shows the enlarged intensity of the 43–45 (°) domain.

The study of the rate capability for the synthesized SAC-spinels was performed by galvanostatic cycling at 25 and 55 °C working temperatures. The discharge current was increased from 1 C until 60 C rate. Fig. 3 gives the evolutions of discharge capacity vs. cycle number registered at different discharge rates for SAC900 at 25 and 55 °C (Fig. 3a and b, respectively) and for SAC1000 at 25 °C (Fig. 3c). Similar evolutions were observed for the others SAC-spinels studied. It is well known that lithium rechargeable batteries need to perform several cycles before reaching a stable regimen of cycling [15,22,25]. Thus, we decided to cycle the cells 50 times at 0.5 C/1 C charge/discharge rates before the rate capability test. It was observed that the maximum capacity (Q_{max}) was reached after a few cycles. As reported in Table 1, at 25 and 55 °C, the experimental Q_{max} for all SAC-spinels is similar (~140 mAh g^{-1} of $LiCr_{0.2}Ni_{0.4}Mn_{1.4}O_4$) being closed to the theoretical capacity (Q_{theo} = 147 mAh g^{-1}). Furthermore, the capacity retention after 50 cycles (QRt-50) is close to 100% for every sample, even at 55 °C. This later performance is remarkable since the main drawback of undoped $LiNi_{0.5}Mn_{1.5}O_4$ is the severe capacity loss when cycling is performed at elevated temperature [12,22,26,27]. We have also tested the cycling performances of the samples SAC950 at 25 °C and SAC900 at 55 °C in the voltage range from 3.4 V to 4.9 V at 0.5 C/1 C charge/discharge rates. This voltage range is one of the most used to test the cycleability of LNMS-based cathodes [22]. The capacity retention determined after 50 cycles has been QRt-50 = 94.91%

Table 1
Unit cell parameter, particle size and electrochemical characteristics (maximum capacity, Q_{max}; coulombic efficieny, CEff; capacity retention after 50 cycles at 1 C discharge rate, QRt-50; discharge capacities at 30 C and 60 C rates) of the SAC-spinels at 25 and 55 °C.

Sample	Cell parameter (Å)	Particle size (nm)	25 °C					55 °C				
			Q_{max} (mAh g^{-1})	CEff (%)	QRt-50 (%)	$Q_{30\,C}$ (mAh g^{-1})	$Q_{60\,C}$ (mAh g^{-1})	Q_{max} (mAh g^{-1})	CEff (%)	QRt-50 (%)	$Q_{30\,C}$ (mAh g^{-1})	$Q_{60\,C}$ (mAh g^{-1})
SAC900	8.1893 (8)	695 (220)	142	93.8	100	136	131	141	94.0	96.94	130	123
SAC950	8.1888 (7)	1080 (260)	140	96.5	98.94	132	123	136	91.6	98.84	120	99
SAC1000	8.1912 (8)	1465 (505)	141	96.4	99.43	118	105	134	94.1	99.26	104	77

Fig. 2. TEM pictures of $LiCr_{0.2}Ni_{0.4}Mn_{1.4}O_4$ spinels annealed at (a) 1000 °C and (b) 950 °C. (c) Particle size histogram of SAC950 sample.

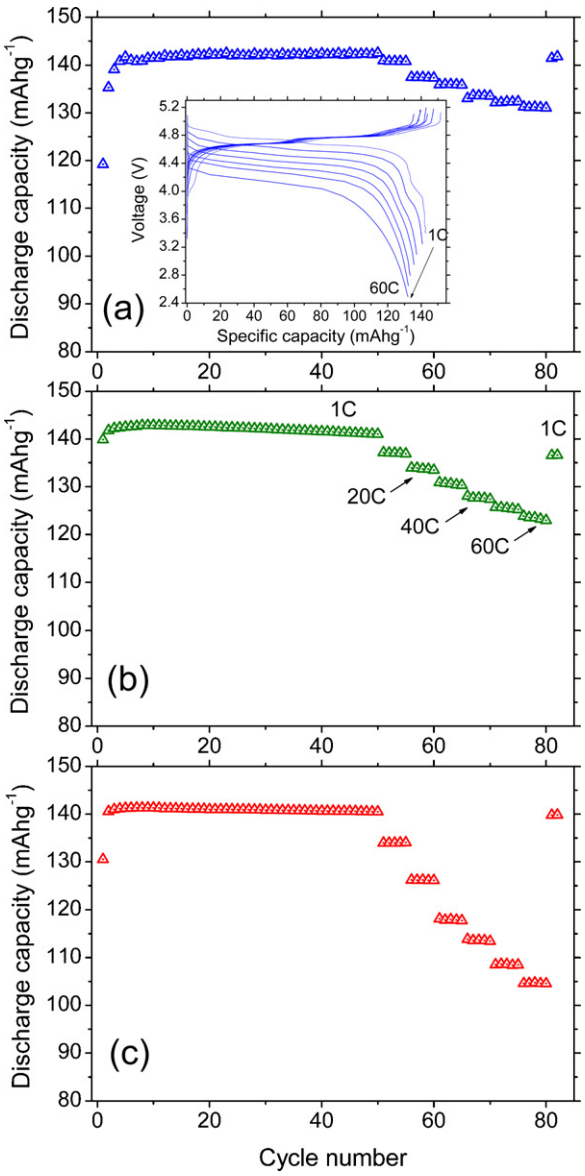

Fig. 3. Evolution of discharge capacity as a function of cycle number at different constant discharge rates for (a) SAC900 at 25 °C, (b) SAC900 at 55 °C, and (c) SAC1000 at 25 °C. The inset in (a) gives the charge/discharge curves of SAC900 at 25 °C registered for different discharge rates (1 C = 147 mA g^{-1}).

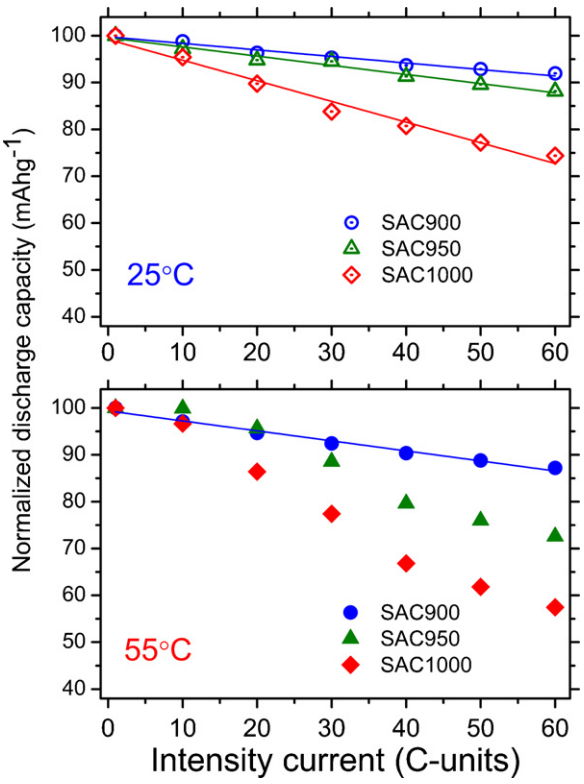

Fig. 4. Evolution of normalized capacity as a function of discharge rate for the SAC-spinels at 25 and 55 °C (1 C = 147 mA g^{-1}).

for SAC900 at 55 °C and 99.54% for SAC950 at 25 °C. These values are close to those obtained when 5.2 V was used as cut-off voltage (Table 1). All these results confirm the remarkable cycling performances of the synthesized SAC-spinels. On the other hand, they show that the end of formation cycling was reached after 50 cycles. So, the cells were ready to the rate capability test.

As shown in Fig. 3a, the discharge capacity (Q_{dch}) of SAC900 at 25 °C slowly decreases from 142 to 131 mAh g^{-1} when the rate increases hardly from 1 C to 60 C. At elevated working temperature (55 °C), Q_{dch} of SAC900 drops from 141 (1 C) to 123 mAh g^{-1} (60 C) (Table 1). Therefore, at the enormous rate of 60 C, the sample SAC900 is able to retain 92 and 86% of Q_{max} when cycled at 25 and 55 °C, respectively. The obtained values confirm the huge rate capability of this spinel, even at elevated temperature [30]. For the SAC1000 sample, which has the biggest particle size (Table 1), the increase of the current rate from 1 C to 60 C induces a capacity loss from 141 to 105 mAh g^{-1} at 25 °C, which corresponds to 74% of capacity retention (Fig. 3c). The whole of these results show that the rate capability of all SAC-spinels is very high and it depends on the annealing and cycling temperatures. It should be noticed that for each rate, no significant capacity loss is observed during the five cycles performed. This result seems to indicate that samples preserve high cycleability for every discharge current until the highest rate of 60 C. To deepen the electrochemical study of the synthesized samples, we presented in the insert of Fig. 3a the voltage–capacity profiles of SAC900 recorded at 25 °C for different rates. During the discharge at 1 C, the curve shows a main plateau in the 5 V-region with three steps ascribed to $Cr^{4+/3+}$ (4.87 V), $Ni^{4+/3+}$ (4.74 V) and $Ni^{3+/2+}$ (4.66 V) redox couples [22,28,31]. With increasing current rate, the three steps overlap in a single plateau and their potential gradually shifts towards lower voltage. These results can be explained by the ohmic voltage drop and the increase of cell polarization at higher currents.

With the aim of better comparing the rate capability of the SAC-spinels at 25 and 55 °C, the evolution of normalized discharge capacity ($Q_{nor} = Q_{dch\text{-}NC} \times 100/Q_{dch\text{-}1\,C}$) with the discharge intensity (*C*-units) is represented in Fig. 4. At 25 °C, note that all samples retain more than 70% of the Q_{max} (Table 1) even at the very fast rate of 60 C. These performances demonstrated that synthesized SAC-spinels exhibit huge rate capability. To our knowledge, the obtained performances have never been reached before for LNMS-based cathodes (Table 2). For instance, capacity retentions of LNMS samples prepared by different methods are 76% at 40 C [32], 87% at 19 C [24], 42% at 15 C [14] and 90% at 10 C [33]. Furthermore, capacity retentions of several SAC-spinels at 25 °C exceed those of optimal nanosized $LiFePO_4$ (58% at 60 C) [5] and $LiCoO_2$ (73% at 50 C) [34]. These exceptional performances make studied SAC-spinels very suitable for high power LIBs.The analysis of the evolution at 25 °C (Fig. 4) shows that Q_{nor} vs. current linearly decreases with the C-rate. The slope of the straight line increases (in absolute value) from −0.14 for SAC900 to −0.20 for SAC950 and then to −0.44 for

Table 2
Electrochemical performances of optimized cathode materials for lithium-ion batteries.

Sample	Synthesis method	Average working voltage (V)	Specific energy (Wh kg^{-1})	Rate capability (capacity retention, %)	Reference
SAC900	Combustion	4.72	670	92% at 60 C	This work
SAC950	Combustion	4.72	660	88% at 60 C	This work
$LiNi_{0.5}Mn_{1.5}O_4$	Resorcinol-formaldehyde	4.7	634	76% at 40 C	[32]
$LiNi_{0.5}Mn_{1.5}O_4$	Pechini	4.7	625	87% at 19 C	[24]
$LiNi_{0.5}Mn_{1.5}O_4$	Polymer assisted	4.7	560	42% at 15 C	[14]
$LiFePO_4$	Off-stoichiometry solid-state	3.4	564	58% at 60 C	[5]
$LiCoO_2$	Hydrothermal	3.9	472	73% at 50 C	[34]

SAC1000. Thus, these results evidenced that lowering the heating temperature of the studied sample improves their rate capability. At 55 °C, a linear decrease of Q_{nor} vs. current is only observed for SAC900, with a slope of −0.21. This slope is slightly higher (in absolute value) than those calculated at 25 °C (slope = −0.14). This indicates that the remarkable rate capability of SAC900 is nearly retained at elevated cycling temperature. For the samples SAC950 and SAC1000, the rate capability is much more affected by the increase of the cycling temperature. For instance, at 60 C the capacity loss of SAC1000 varies from 25% at 25 °C to 43% at 55 °C.

It has been widely reported that particle size is an important parameter which affects the electrochemical performances of electrode materials, especially at high discharge rates [3,13,15,24,27,34]. As has been previously concluded, the cubic spinel structure of the SAC-samples remains unchanged from 900 to 1000 °C being the growing of the particle size, the main effect when the annealing temperature is raised. Fig. 5 gives the variation of Q_{dch} with the particle size for different rates at 25 and 55 °C. At 25 °C and for 1 C, there is no significant influence of the particle size on the discharge capacity ($Q_{dch} \sim 140$ mAh g^{-1}). For faster rates, the effect of the particle size is evident. Indeed, for SAC900, with the smallest particle size (695 nm), Q_{dch} slowly decreases from 142 (1 C) to 131 mAh g^{-1} (60 C). Whereas, for SAC1000, having the biggest particles (1465 nm) Q_{dch} decreases more from 141 (1 C) to 105 mAh g^{-1} (60 C). Li^+-ion diffusion from/into the electrodes is one the main factor limiting the kinetics of redox reactions in LIBs [3,5,22,32]. In our case, it can be assume that the diffusion coefficient of all SAC-samples is similar because of the spinel structure is not modified on heating. According to Einstein–Smoluchowski law, the time (t) required for fully diffusion of Li^+ ions from the surface to the center of the particles is $t = d^2/2D$, where d is the particle radius and D is the diffusion coefficient. As the discharge capacity of all samples is similar and close to Q_{theo} for 1 C, 1 h is enough to fully insert Li^+ into the SAC-spinels, even for SAC1000 with the biggest particle size. Nevertheless, when the rate became faster, the Li^+-insertion reaction has not enough time to be fulfilled. This explains the capacity loss observed on increasing the rate. Obviously, this effect is more pronounced for samples having bigger particle size as it is clearly shown in Fig. 5. At 55 °C, the evolution of Q_{dch} vs. particle size follows a similar tendency evidenced at 25 °C. Note that the decrease of discharge capacity with the rate is more pronounced at 55 °C for each sample. For instance, in the case of SAC1000 (1465 nm), the percent of Q_{dch} loss between 1 C and 60 C rate is 25% at 25 °C and 43% at 55 °C. A similar behaviour was reported by Kim et al. for a $LiNi_{0.5}Mn_{1.5}O_4$ sample prepared by the molten salt method [35]. For this LNMS-sample, the Q_{dch} loss was 4% at 30 °C for 0.14 C while it reaches 17% at 55 °C for 3 C. In Table 1, the coulombic efficiency (CEff) at 25 and 55 °C for the synthesized SAC-spinels are summarized. The CEff-values correspond to the cycle at which the maximum discharge capacity was reached. They was calculated as $CEff = Q_{dch\text{-}max} \times 100/Q_{ch\text{-}max}$. In all cases, the coulombic efficiency is elevated (>90% at 25 and 55 °C). Nevertheless, as CEff does not reach the value of 100%, Q_{ch} is always higher than Q_{dch}. This behaviour can be explained by the oxidation of the electrolyte at the high potentials reached on charging. Electrolyte degradation gives way to the formation of a corrupted solid electrolyte interface which increases the cell impedance [28]. Data in Table 1 shown that CEff-values at 25 °C are higher than those at 55 °C, i.e. the electrolyte degradation is bigger at elevated temperature. This experimental result can justify the decrease of the rate capability of the SAC-spinels on increasing the working temperature.

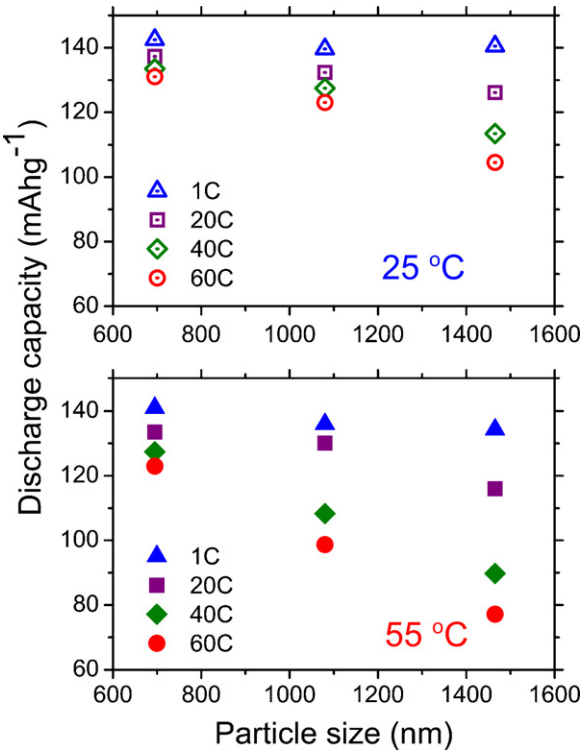

Fig. 5. Evolution of the rate capability as a function of the particle size at 25 and 55 °C.

The technological interest of electrode materials able to deliver high capacity at high current resides in the fact that they permit to develop rechargeable batteries with power densities as high as those of supercapacitors [4–6]. In Fig. 6, Ragone plots for the SAC-spinels at 25 and 55 °C are shown. The specific power (P) was calculated according to $P = W t^{-1}{}_{dch}$ where W, in Wh kg^{-1} of $LiCr_{0.2}Ni_{0.4}Mn_{1.4}O_4$, is the specific energy calculated by integrating the E vs. Q_{dch} curves and t_{dch} is the total discharge time. The well-established inverse relationship between specific energy and specific power is observed. It is important to remark that all SAC-spinels are able to deliver more than 10,000 W kg^{-1} of $LiCr_{0.2}Ni_{0.4}Mn_{1.4}O_4$ even at elevated temperature. These outstanding power performances are among the reported for the electrochemical capacitors [4–6]. The fact that such spinels can drain power densities similar to those of supercapacitors is

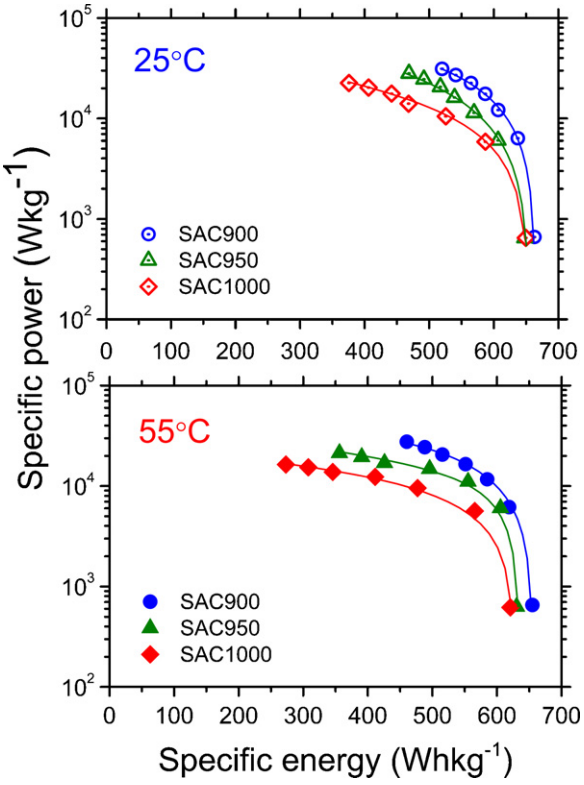

Fig. 6. Ragone plot of SAC-spinel at 25 and 55 °C.

consistent with their fast bulk Li^+-insertion. Finally to indicate that among the synthesized samples, SAC900 exhibits the best electrochemical properties (Table 2). In fact, it is able to deliver 31,000 W kg^{-1} keeping a specific energy of 520 Wh kg^{-1} at 25 °C and 27,500 W kg^{-1} with 460 Wh kg^{-1} at 55 °C. These outstanding electrochemical performances show that the $LiCr_{0.2}Ni_{0.4}Mn_{1.4}O_4$ spinel synthesized at 900 °C is a really promising cathode for high-power Li-ion batteries needed to power hybrid and electric vehicles.

4. Conclusion

$LiCr_{0.2}Ni_{0.4}Mn_{1.4}O_4$ cathode materials have been prepared by the sucrose aided combustion method followed by thermal treatments at 900, 950 and 1000 °C. The structural study shows that SAC-samples are single-phase cubic spinel. They have similar unit cell parameter ($a_c \sim 8.189$ Å) indicating that there is no structural modification on heating. The morphological characterization by TEM evidences that the main effect of the thermal treatment is the remarkable growth of the particle size from 695 nm at 900 °C to 1465 nm at 1000 °C. The galvanostatic cycling data registered at 25 and 55 °C shows that the working voltage of all SAC-spinels is very high (~4.7 V) being similar their experimental discharge capacity (~140 mAh g^{-1}) and close to the theoretical one (147 mAh g^{-1}). Furthermore, their capacity retention after 50 cycles is close to 100% even at elevated cycling temperature. It shows the excellent cycling performances of synthesized Cr-doped LNMS. At 25 °C, all samples keep more than 70% of Q_{max} until the very fast rate of 60 C. This retention value demonstrated that SAC-spinels have huge rate capability. To the best of our knowledge, they exhibit the highest rate capability reported for LNMS-based cathodes to date. The study of the role of the particle size on the rate capability of the SAC-spinels at 25 and at 55 °C shows that the rate capability is enhanced on decreasing the particle size at both temperatures. Among the samples synthesized, the SAC900 exhibits the best electrochemical properties. This sample keeps 92% of Q_{max} for 60 C at 25 °C, and 87% at 55 °C. It is able to store 663 Wh kg^{-1} and deliver 31,000 W kg^{-1} at 25 °C, and 654 Wh kg^{-1} and 27,500 W kg^{-1} at 55 °C. These outstanding electrochemical performances make the $LiCr_{0.2}Ni_{0.4}Mn_{1.4}O_4$ synthesized at 900 °C one of the most promising cathode materials for practical high-power Li-ion battery.

Acknowledgments

Financial support through the projects MAT2008-03182 (MICINN), MATERYENER P2009/PPQ-1626 (CAM) and 2009MA0007 (CSIC/CNRST) are gratefully recognized. M. Aklalouch thanks the AECI for the MAEC-AECI fellowship.

References

[1] G. Pistoia (Ed.), Electric and Hybrid Vehicles, Elsevier, 2010.
[2] M. Armand, J.M. Tarascon, Nature 451 (2008) 652.
[3] P.G. Bruce, B. Scrosati, J.M. Tarascon, Angew. Chem. 47 (2008) 2930.
[4] P. Simon, Y. Gogotsi, Nat. Mater. 7 (2008) 845.
[5] B. Kang, G. Ceder, Nature 458 (2009) 190.
[6] S.W. Lee, N. Yabuuchi, B.M. Gallant, S. Chen, B.-S. Kim, P.T. Hammond, Y. Shao-Horn, Nat. Nanotechnol. 5 (2010) 531.
[7] C. Delmas, I. Saadoune, Solid State Ion. 53–56 (1992) 370.
[8] L. Wang, J. Li, X. He, W. Pu, C. Wan, C. Jiang, J. Solid State Electrochem. 13 (2009) 1157.
[9] M.M. Thackeray, Prog. Solid State Chem. 25 (1997).
[10] J.M. Amarilla, K. Petrov, F. Picó, G. Avdeev, J.M. Rojo, R.M. Rojas, J. Power Sources 191 (2009) 591.
[11] R. Dominko, M. Bele, M. Gaberscek, M. Remskar, D. Hanzel, S. Pejovnik, J. Jamnika, J. Electrochem. Soc. 152 (2005) A607.
[12] Y.K. Sun, Y.S. Lee, M. Yoshio, K. Amine, Electrochem. Solid State Lett. 5 (2002) A99.
[13] L. Pascual, H. Gadjov, D. Kovacheva, K. Petrov, P. Herrero, J.M. Amarilla, R.M. Rojas, J.M. Rojo, J. Electrochem. Soc. 152 (2005) A301.
[14] J.C. Arrebola, A. Caballero, M. Cruz, L. Hernán, J. Morales, E. Rodríguez Castellón, Adv. Funct. Mater. 16 (2006) 1904.
[15] X. Fang, Y. Lu, N. Ding, X.Y. Feng, C. Liu, C.H. Chen, Electrochim. Acta 55 (2010) 832.
[16] C. Li, H.P. Zhang, L.J. Fu, H. Liu, Y.P. Wua, E. Rahm, R. Holze, H.Q. Wu, Electrochim. Acta 51 (2006) 3872.
[17] J.M. Amarilla, R.M. Rojas, F. Pico, L. Pascual, K. Petrov, D. Kovacheva, M.G. Lazarraga, I. Lejona, J.M. Rojo, J. Power Sources 174 (2007) 1212.
[18] N. Kawai, T. Nakamura, Y. Yamada, M. Tabuchi, J. Power Sources 196 (2011) 6969.
[19] Q. Zhong, A. Bonakdarpour, M. Zhang, Y. Gao, J.R. Dahn, J. Electrochem. Soc. 144 (1997) 205.
[20] R.M. Rojas, J.M. Amarilla, L. Pascual, J.M. Rojo, D. Kovacheva, K. Petrov, J. Power Sources 160 (2006) 529.
[21] L.H. Chi, N.N. Dinh, S. Brutti, B. Scrosati, Electrochim. Acta 55 (2010) 5110.
[22] G.Q. Liu, L. Wen, Y.M. Liu, J. Solid State Electrochem. 14 (2010) 2191.
[23] H. Wang, T.A. Tan, P. Yang, M.O. Lai, L. Lu, J. Phys. Chem. C 115 (2011) 6102.
[24] M. Kunduraci, J. Al-Sharab, G.G. Amatucci, Chem. Mater. 18 (2006) 3585.
[25] J.M. Amarilla, R.M. Rojas, J.M. Rojo, J. Power Sources 196 (2011) 5951.
[26] R. Alcantara, M. Jaraba, P. Lavela, J.L. Tirado, J. Electroanal. Chem. 566 (2004) 187.
[27] M. Aklalouch, R.M. Rojas, J.M. Rojo, I. Saadoune, J.M. Amarilla, Electrochim. Acta 54 (2009) 7542.
[28] M. Aklalouch, J.M. Amarilla, R.M. Rojas, I. Saadoune, J.M. Rojo, J. Power Sources 185 (2008) 501.
[29] M.D. Abramoff, P.J. Magelhaes, S.J. Ram, Biophoton. Int. 11 (2004) 36.
[30] M. Aklalouch, J.M. Amarilla, R.M. Rojas, I. Saadoune, J.M. Rojo, Electrochem. Commun. 12 (2010) 548.
[31] Y. Terada, K. Yasaka, F. Nishikawa, T. Konishi, M. Yoshio, I. Nakai, J. Solid State Chem. 156 (2001) 286.
[32] K.M. Shaju, P.G. Bruce, Dalton Trans. (2008) 5471.
[33] H.M. Wu, I. Belharouak, H. Deng, A. Abouimrane, Y.-K. Sun, K. Amine, J. Electrochem. Soc. 156 (2009) A1047.
[34] M. Okubo, E. Hosono, J. Kim, M. Enomoto, N. Kojima, T. Kudo, H. Zhou, I. Honma, J. Am. Chem. Soc. 129 (2007) 7444.
[35] J.H. Kim, S.T. Myung, C.S. Yoon, S.G. Kang, Y-K. Sun, Chem. Mater. 16 (2004) 906.